

## **MICROCRACKING BEHAVIOR AND SOFTENING PROPERTIES OF CONCRETE**

H. Mihashi, K. Kirikoshi and N. Nomura  
Dept. of Architecture and Building Science, Tohoku University, Sendai,  
Japan  
K. Otsuka  
Dept. of Civil Engineering, Tohoku Gakuin University, Tagajyo, Japan  
Y. Kaneko  
Div. of Structural Design, Shimizu Co., Tokyo, Japan

### **Abstract**

In this paper, influence of aggregates on tension softening diagram of concrete is presented. Compact tension tests were carried out on concrete and the load versus CMOD curves were analyzed by a poly-linear approximation method. Concrete specimens containing aggregates of two types and five different sizes were tested. In addition, two types of specimens were tested to study the influence of the thickness. Detailed cracking behavior was also observed by means of a unique x-ray technique using contrast medium. The main conclusion of this paper is that not only the size of aggregates but the shape influence the characteristics of fracture process zone and the tension softening diagram. Keywords: Microcracking, fracture process zone, tension softening diagram, x-ray technique, aggregate size, aggregate type.

### **1 Introduction**

For numerical simulation of nonlinear behavior of concrete structures due to cracking, fracture mechanics has been widely used. The constitutive law to describe the behavior of concrete under tension, however, is sometimes too simple. It is no doubt the energy consumption in an equivalent crack system is the most important concept by which fracture

---

mechanics of concrete can contribute to structural engineering, and the exact physical explanation on the softening property is not important to usual structural analyses. However, more detailed information about the softening diagram is also necessary especially for the purpose of studying the failure mechanism of concrete structures including the deterioration and of developing new materials and/or construction systems, since the shape of the tension softening diagram influences the behavior of concrete structures in which cracking is dominant. So far, quite few papers have been published to discuss the relation between directly observed microcracking behavior and the tension softening diagram, though there are a lot of papers published discussing the softening diagram.

Heterogeneous material structure of concrete influences to a great extent the microcracking behavior. Because of the heterogeneity, fracture process zone (FPZ) is created which corresponds to a microcracked zone with some remaining ligaments for stress transfer (Hillerborg et al. 1976). While there is a general agreement that FPZ exists in concrete, no agreement has been obtained on exactly what constitutes FPZ in cementitious materials (Mindess 1991). Although various experimental techniques have been developed and applied to identify the extent of FPZ, the obtained values are dependent on the capacity of adopted techniques and sometimes contradict one another.

Since cracking in concrete is a three dimensional phenomena, surface crack measurement is usually inadequate. Mihashi et al. (1991, 1992) reported on the microcracking properties of concrete studied by means of a three-dimensional acoustic emission technique. They found that a microcracking zone developed around a visible macrocrack and that the width of FPZ vertical to the main cracking was about three times the maximum size of the aggregates in the concrete. Schlangen and van Mier (1991) adopted a vacuum impregnation technique and observed the sliced surfaces after impregnation at various loading stages to determine the internal crack geometry. They pointed out the softening of concrete under tensile stress was mainly due to crack face bridging in the wake of the macrocrack tip.

Otsuka (1989) developed a new crack detection technique using x-ray and contrast medium, which is powerful to detect fine cracks formed in concrete. He used this unique technique to evaluate FPZ to reveal the relation between the size and shape of FPZ and the maximum aggregate size, and the size of test specimens (Otsuka 1992, Otsuka et al. 1993 and Otsuka 1994). He concluded that size of FPZ is strongly related to the maximum aggregate size and that the fracture energy per unit projected area:  $G_F$  increases as the maximum aggregate size becomes larger, though the fracture energy per unit volume of FPZ:  $W_F$  is almost constant independently of the maximum aggregate size.

In the present paper, influence of aggregates on tension softening

diagram of concrete is discussed. Compact tension tests are carried out on concrete and the load-CMOD curves are analyzed by a poly-linear approximation method (Uchida et al. 1995). Two types and totally five different sizes of aggregates are tested. In addition, two types of specimens were tested to study the influence of the thickness of specimens. Detailed FPZ observed by means of the x-ray technique was also related to the softening diagram. On the basis of these results, characteristics of FPZ are clarified as a function of aggregate's type and size. Then the mechanism to enhance the cracking resistance in concrete is discussed from the view point of softening properties.

## 2 Experiments

### 2.1 Crack detection technique with x-ray and contrast medium

The unique crack detection technique developed by Otsuka (1989) consists of injecting a contrast medium into holes embedded in the specimen, and taking radiographs at certain stages of loading directly on x-ray films and/or continuously by video camera using a x-ray image amplifier. Further details are described in Otsuka (1989, 1992 and 1994) and Otsuka et al. (1993).

### 2.2 Material and specimens

#### 2.2.1 Specimen geometry and test set-up

Compact tension specimens of two different sizes as shown in Fig. 1 were used and the dimension for both types is given in Table 1. Notches were

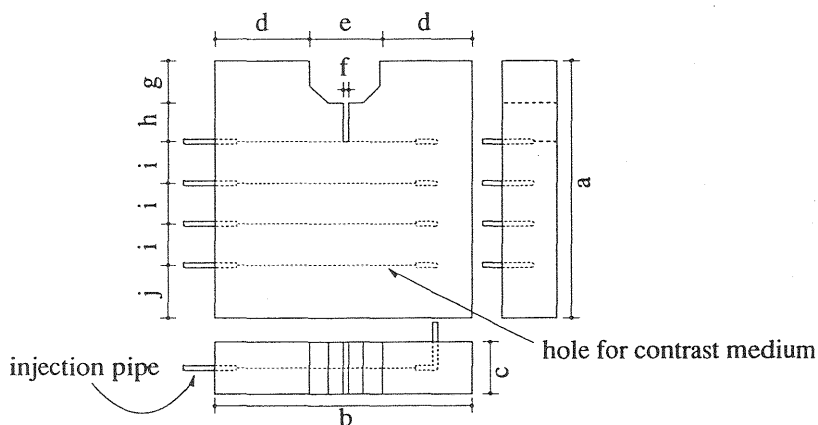


Fig. 1 Geometry of specimens

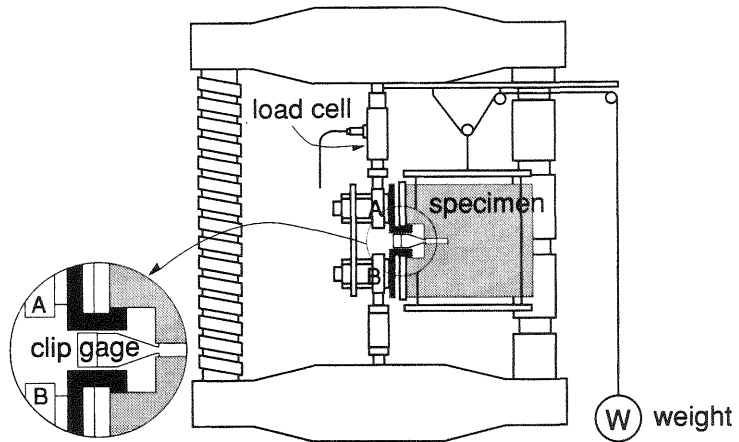


Fig. 2 Test set-up

sawn by a diamond cutter. Fig. 2 shows the test set-up for the compact tension test. Two steel plates were glued to the specimen to fix the loading equipment (A & B in Fig. 2) and self-weight of the specimen was canceled by the weight (W in Fig. 2).

### 2.2.2 Preparation of specimens

Concrete used for casting the specimens was made with high-early strength Portland cement and different types and sizes of aggregates (Table 2). The mix proportions are shown in Table 3. Water-cement ratio was 0.5 for all test series. Fine aggregate was river sand with the maximum size of 5 mm. Coarse aggregates were crushed stone for Series C and river gravel for Series G. Load and CMOD were measured

Table 1 Dimension of Specimens

	a	b	c	d	e	f	g	h	I	j
Type A	250	250	50	90	60	3	30	50	40	50
Type B	350	350	90	145	60	3	30	120	50	40

Table 2 Test series

	Aggr. Type	Max Aggr. Size ( $d_{max}$ )	Specimen Type
Series C	crushed stone	10, 15, 20	A & B
Series G	river gravel	5, 10, 15, 20 & (25)**	A*

\*B was used only for mortar

\*\*only one case different from others

Table 3 Concrete composition (kg/m<sup>3</sup>) and compressive strength (MPa)

Test Series	C10	C15	C20	M05	G10	G15	G20	G25
Cement	408	398	388	402	390	380	370	350
Aggregate								
0 - 5	872	817	762	2,338	1,646	1,402	1,278	1,173
5 - 10	761	420	369	0	1,360	650	468	308
10 - 15	0	420	548	0	0	810	468	460
15 - 20	0	0	548	0	0	0	626	460
20 - 25	0	0	0	0	0	0	0	460
Water	204	199	194	201	195	190	185	175
Comp.Str.	29.8	33.0	35.2	32.6	25.9	26.5	28.3	24.2

Table 4 Width of FPZ (Otsuka et al. 1993)

	C10	C15	C20	M05	G10	G15	G20	G25
VL	13	15	22	13	16	17	26	25
VL <sub>max</sub>	22	24	31	20	29	27	38	44

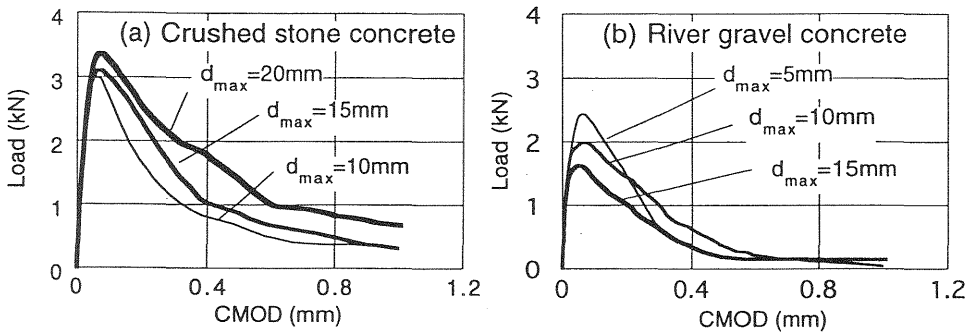


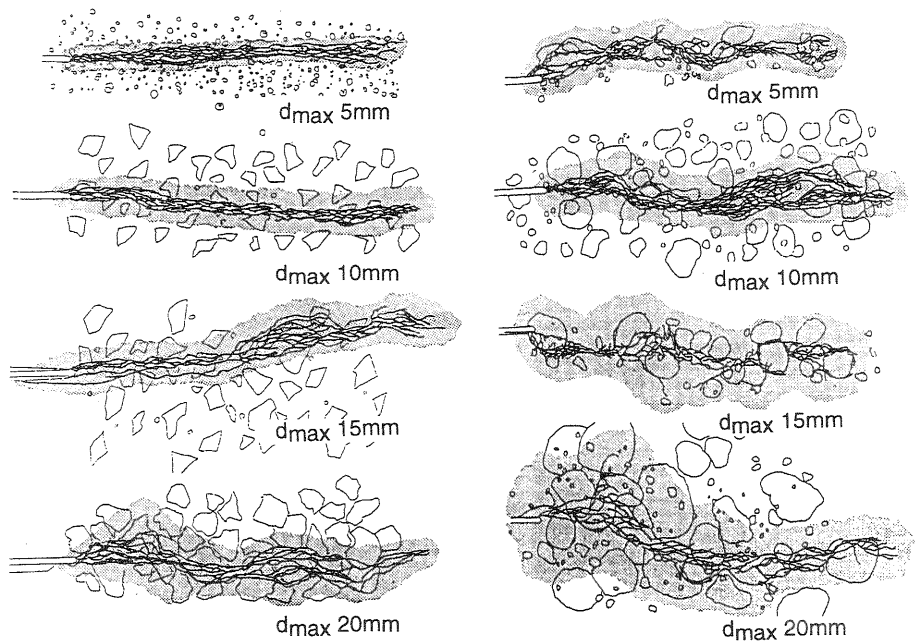
Fig. 3 Typical load vs. CMOD curves

by a load cell and clip gage. Specimens were cured in water of 20°C until days of loading test.

### 2.3 Characteristics of cracking properties and FPZ

Typical load versus CMOD curves of Type A specimens are shown in Fig. 3. Fig. 4 shows the influence of the maximum aggregate size ( $d_{max}$ ) on the shape of FPZ at the final stage. In these figures, fine cracks are drawn with solid lines and microcracking zones are described as slightly dark areas. The maximum vertical width of damaged zone with fine cracks (VL) and that of microcracking zone (VL<sub>max</sub>) are shown in Table 4. These values were obtained as the mean values of results observed in mostly three specimens (Otsuka et al. 1993).

It is clearly shown that the width of FPZ becomes wider as the



(a) Crushed stone concrete      (b) River gravel concrete  
 Fig. 4 Typical FPZ of concrete detected by x-ray technique

maximum aggregate size is larger. This result coincides with those obtained in the previous studies (Mihashi et al. 1991 & 1992, Schlagen et al. 1991). However the width of FPZ of crushed stone concrete is much narrower than that of river gravel concrete. In case of crushed stone concrete, many fine cracks passed through aggregates. On the other hand, fine cracks propagated in zigzag lines around aggregates in case of river gravel concrete.

### 3 Determination of tension softening diagram

#### 3.1 Poly-linear approximation method

A poly-linear approximation method to determine the tension softening diagram was proposed by Kitsutaka et al. (1994). This method is of a kind of inverse analysis which determines the tension softening diagram of concrete from the load-displacement curve on the basis of the fictitious crack model (Hillerborg et al. 1976). In this method, the softening diagram is approximated by the poly-linear diagram and the coordinate of each point of the softening diagram is determined step by step with the

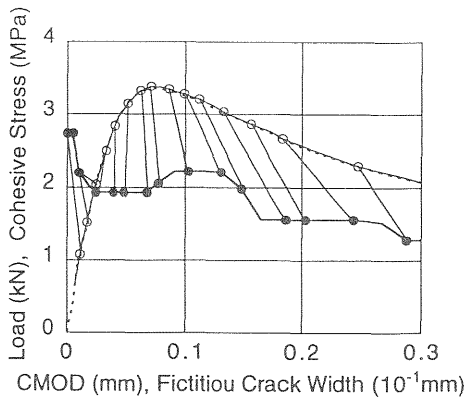


Fig. 5 Example of poly-linear softening diagram and corresponding load vs. CMOD.

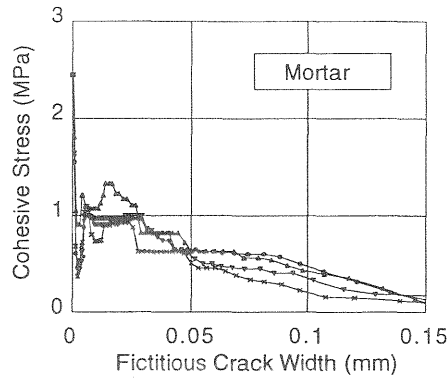


Fig. 6 Softening diagrams of mortar (Type A/ M05)

development of the fictitious crack in the analysis. Uchida et al. (1995) developed a finite element code on the basis of Kitsutaka's method. In the present study, tension softening diagrams of mortar and concrete were determined by means of the finite element code from load versus CMOD curves shown in Fig. 3.

### 3.2 Results and discussion

Fig. 5 shows an example of the load versus CMOD curve and the corresponding tension softening diagram determined by the poly-linear approximation method. Open circles on the load-displacement curve were calculated from the softening diagram and the broken line was the experimental result. Softening in a region near the notch tip initiated already around the 1/3 of the maximum load and it extends much further when the loading level reaches the peak.

Fig. 6 shows softening diagrams determined for mortar specimens of Type A. There is a scatter among four specimens but it can be possible to describe the softening diagram by a trilinear relation between the cohesive stress and the fictitious crack width. Just after the softening initiates, a very steep descending branch is observed. Then after a plateau, the second descending branch starts which is much more gently sloping.

Figs. 7 and 8 show the influence of  $d_{max}$  on the strain softening diagram in cases of crushed stone concrete and of river gravel concrete, respectively. There is a tendency that the area under the diagram increases as  $d_{max}$  becomes larger. It is also observed that the cohesive stress level in case of crushed stone concrete is higher than that in case of river gravel concrete for the same size of the maximum aggregates.

Comparison between Fig.7 and Fig.8 may lead to a following findings. When  $d_{max}$  is larger than 15mm, shape of the softening diagram is

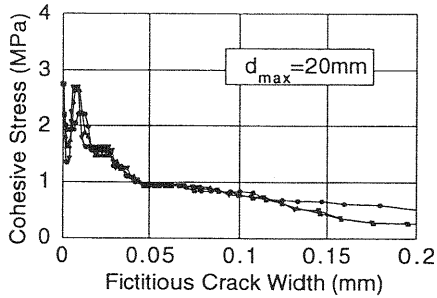
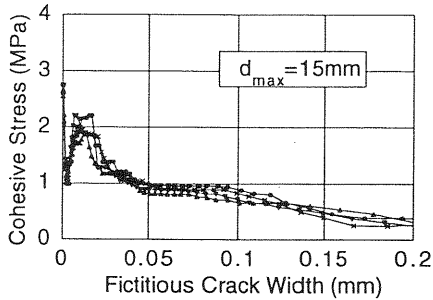
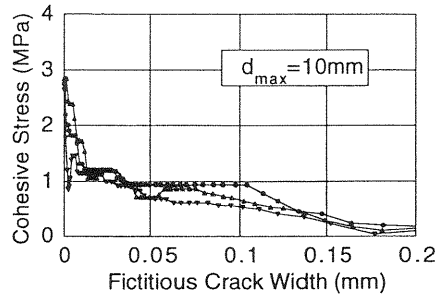


Fig. 7 Softening diagrams of crushed stone concrete

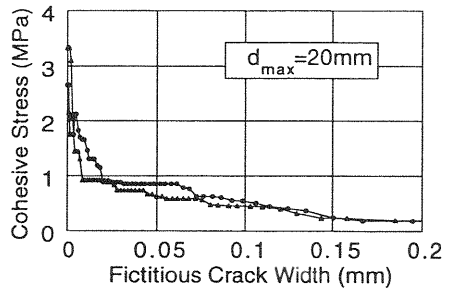
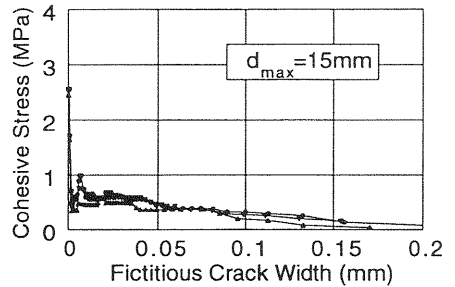
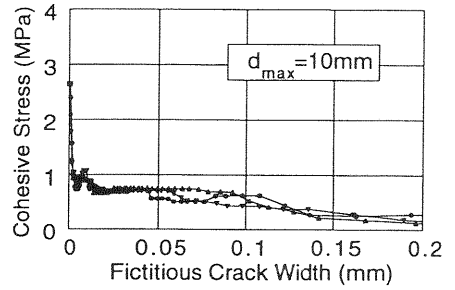


Fig. 8 Softening diagrams of river gravel concrete

obviously influenced by the type of aggregates. In case of crushed stone concrete ( $d_{max} \geq 15$  mm), a valley portion is formed after the first descending branch and then a peak is formulated. After the peak, the relation can be described by a trilinear diagram. The descending branch after the peak is much gentler than that of the first descending branch. On the other hand, the whole softening diagrams of the river gravel concrete can be described by a trilinear diagram independently of  $d_{max}$ . This difference might be caused by the different cracking properties. In other words, crushed stone often works as a crack arrester by the bridging mechanism in a similar way to some kinds of fibers in fiber reinforced concrete (Uchida et al. 1995).

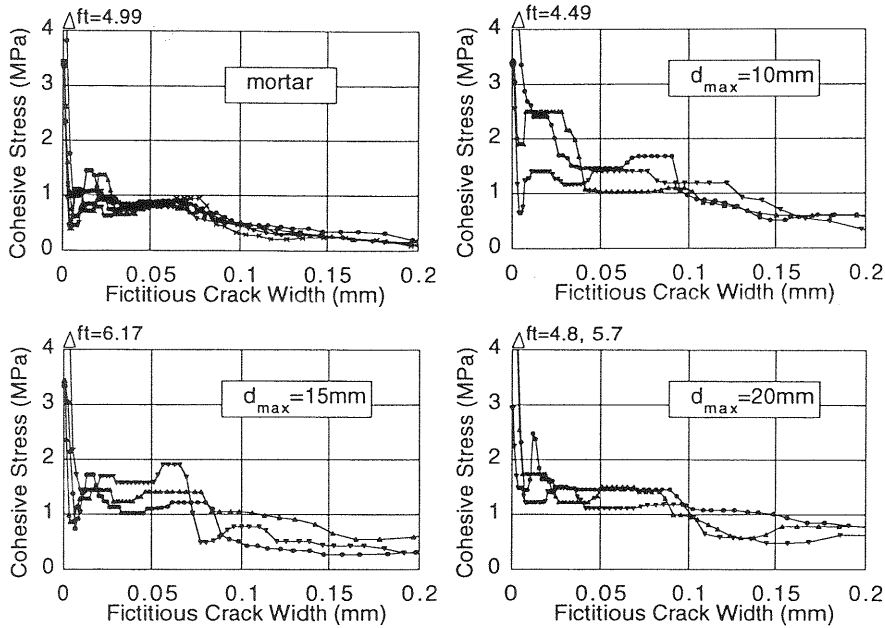


Fig. 9 Softening diagrams of crushed stone concrete [Type B specimens]

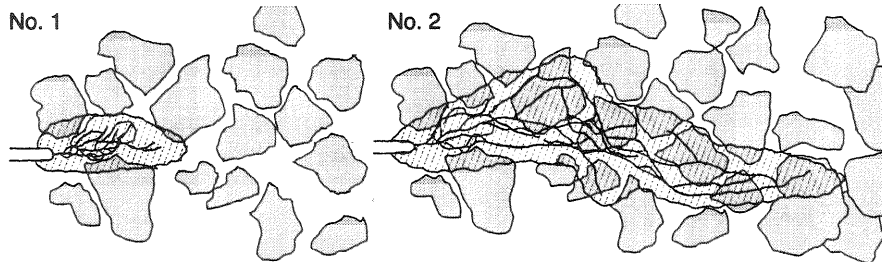


Fig. 10 Microcracking behavior in crushed stone concrete [A-C20].

In case of thicker specimens such as Type B specimens, the peak becomes much less obvious but the global softening behavior is close to a trilinear diagram while the cohesive stress level of the plateau is higher than that of both types of concrete of thinner specimens. Moreover the length of the plateau is longer, too (Fig. 9).

Figs. 10 and 11 show examples of detailed observation of the fracture

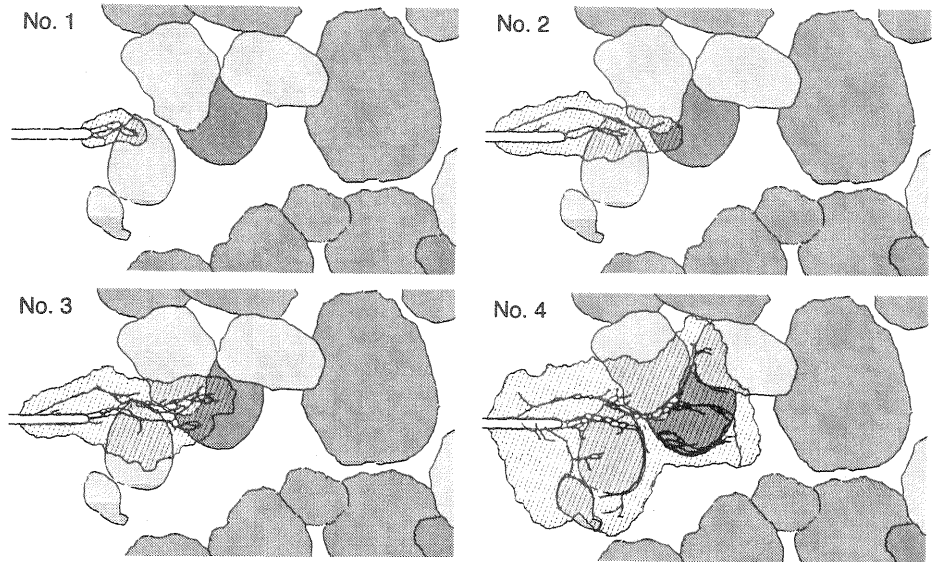


Fig. 11 Microcracking in river gravel concrete [A-G25].

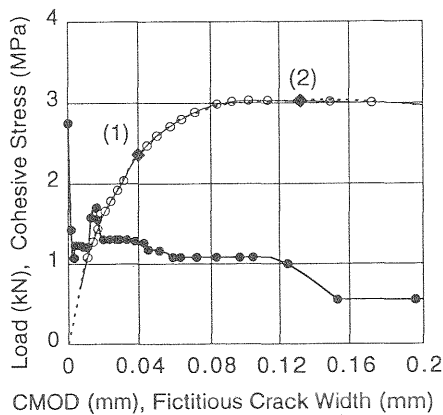


Fig. 12 Load vs. CMOD and softening diagram [A-G25]

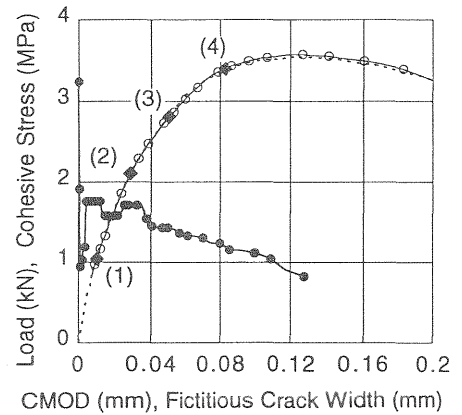


Fig. 13 Load vs. CMOD and softening diagram [A-C20]

process and microcracking in a crushed stone concrete: [A-C20] and in a river gravel concrete: [A-G25], respectively. In Fig. 10, the first crack initiated from the notch tip passed through an aggregate located near the notch tip, though the size of the aggregate is rather small. On the other hand, the first crack shown in Fig. 11 was arrested by an aggregate and then another crack initiated from a portion distant from the notch tip. This grows as the second and main crack. It means microcracking behavior is a highly random phenomenon that is dependent upon not only the size, shape and type of aggregates but the spacial arrangement.

Figs. 12 and 13 show load versus CMOD curves and the corresponding softening diagrams of a crushed stone concrete and river gravel concrete, respectively. Number on the curve is corresponding to that in figures of fracture process and microcracking shown in Figs. 10 and 11. It is noticeable that the tension softening diagram of the river gravel concrete has a valley after the steep descending branch.

#### 4 Conclusions

Microcracking behavior was observed by means of a unique x-ray technique and the result was related to characteristics of the tension softening diagram of concrete. Especially it was clarified that crack arresting mechanism may enhance the cracking resistance in concrete. It is the reason why crushed stone concrete usually shows a higher resistance to cracking than that of river gravel concrete.

#### 5 Acknowledgement

Authors would like to thank Prof. K. Rokugo, Prof. Y. Uchida and Mr. Kurihara of Gifu University for their kind offer of the finite element code to determine the poly-linear softening diagrams.

#### 6 References

- Hillerborg, A., Modeer, M. and Petersson, P.E. (1976) Analysis of crack formation and crack growth in concrete by means of fracture mechanics and finite elements. **Cem. & Concr. Res.**, 6, 773-782.
- Kitsutaka, Y., Kamimura, K. and Nakamura, S. (1994) Evaluation of aggregate properties on tension softening behaviour of high strength concrete, in **High Performance Concrete**, ACI SP149-40, 711-727.
- Mihashi, H., Nomura, N. and Niiseki, S. (1991) Influence of aggregate size on fracture process zone of concrete detected with three dimensional acoustic emission technique, **Cem. & Concr. Res.**, 21, 737-744.
- Mihashi, H. and Nomura, N. (1992) Microcracking and tension-softening properties of concrete, **Cem. & Concr. Comp.**, 14, 91-103.
- Mindess, S. (1991) Fracture process zone detection, in **Fracture**

---

**Mechanics - Test Methods for Concrete** (eds. S.P. Shah and A. Carpinteri), Chapman and Hall, 231-261.

Otsuka, K. (1989) X-ray technique with contrast medium to detect fine cracks in reinforced concrete, in **Fracture Toughness and Fracture Energy** (eds. H. Mihashi, H. Takahashi and F.H. Wittmann), Balkema, 521-534.

Otsuka, K. (1992) Detection of fracture process zone in concrete by means of x-ray with contrast medium, in **Fracture Mechanics of Concrete Structures** (ed. Z.P. Bazant), Elsevier Applied Science, 485-490.

Otsuka, K. and Katsube, H. (1993) Influences of aggregate size on the behavior of fracture process zone in concrete, **J. JSCE**, 478/V-21, 109-116. (In Japanese)

Otsuka, K. (1994) Size effect in fracture process zone of concrete, in **Size Effect in Concrete Structures** (eds. H. Mihashi, H. Okamura and Z.P. Bazant), E & FN Spon, 47-56.

Schlangen, E. and van Mier, J.G.M. (1991) **Experimental and Numerical Analysis of Micromechanisms of Fracture of Cementbased Composites**, Report 25.5-91-1/VFC, Delft Univ. of Technology, 28p.

Uchida, Y., Kurihara, N., Rokugo, K. And Koyanagi, W. (1995) Determination of tension softening diagrams of various kinds of concrete by means of numerical analysis, in **Fracture Mechanics of Concrete Structures** (ed. F.H. Wittmann), Aedificatio Publishers, 1, 17-30.